科技部補助

大專學生研究計畫研究成果報告

計畫名稱：黏液蛋白醣化酵素修飾 ErbB2 受器進而調節脂肪幹細胞分化為類許旺氏細胞應用於周邊神經再生之研究

執行計畫學生：林昱達

學生計畫編號：MOST 106-2813-C-040-024-B
研究期間：106 年 07 月 01 日至 107 年 02 月 28 日止，計 8 個月

指導教授：廖玟潔

處理方式：本計畫涉及專利或其他智慧財產權，2 年後可公開查詢

執行單位：中山醫學大學醫學系解剖學科

中華民國 107 年 03 月 26 日

Abstract

Brachial plexus injury is one of the major causes of disability. End-to-end neurorrhaphy (EEN) promotes recipient nerve recovery and preserves donor functions. However, axon sprouting of motor neuron from the cell body to target muscles is the most time-consuming. The recovery process relies on the proliferation and migration of Schwann cells (SCs). Adipose tissue-derived stem cells (ADSCs) have the potential to differentiate into Schwann-like cells (Scis) by treatment with multiple growth factors. Mucin-type O-glycosylation can regulate growth factor-receptor tyrosine kinase (RTK) signalling during ADSC differentiation. However, the functions of O-glycosylation in ADSC differentiation and nerve regeneration are largely unknown. This study used ADSCs to examine the changes in O-glycans on human epidermal growth factor receptor 2 (ErbB2) and determine the effects of differentiated ADSCs in an EEN model. Q-PCR was used to study the role of the gene expression of O-glycosyltransferases (N-acetylgalactosaminyltransferase, GALNT). Lectin pull-down assays were used to analyse O-glycans on growth factor receptors in ADSCs. The implantation of ADSCs and Schwann-like cells (Scis) was used to treat peripheral nerve injury. At one and three months after surgery, the regenerating nerve tissues were processed for investigation.

The results from this project provide new information about the change and function of the O-glycosylation on growth factor receptor, ErbB2, during the differentiation of ADSCs into Scis. Additionally, this study helps us understand if differentiated ADSCs has a synergistic effect in promoting nerve regeneration.

Introduction

Peripheral nerve injury (PNI) is one of the most common injuries around the world (Evans 2001). Most traumatic brachial plexus injuries (BPI) occur when the arm is forcefully pulled or stretched. BPI typically occurs during the most active years in people's lives, and it results in weakness or numbness, loss of sensation, and loss of

movement (Ciaramitaro et al. 2010). Since 1992, end-to-end neurorrhaphy (EEN) has been used in various nerve repair strategies (Papalia et al. 2007; Viterbo et al. 1992) Regeneration, conduction and muscular function restoration of the injured peripheral axons takes a long time, approximately one to three months (Liao et al. 2009, 2010). During nerve regeneration, neurotrophins are secreted by nerve target cells (muscle cells), the surrounding glia and Schwann cells (SCs), which lead the way in guiding nerve terminal sprouting (Chen et al. 2007; J W Faweett and Keynes 1990; Son and Thompson 1995b, a). SCs revert to immature states to proliferate and guide regenerating axons by secreting neurotrophic factors, such as neuregulins, nerve growth factor (NGF), brain-derived neurotrophic factor (BDNF), neurotrophin-3 (NT3), ciliary neurotrophic factor (CNTF), and glial cell line-derived neurotrophic factor (GDNF) (Carroll et al. 1997; Davis and Stroobant 1990; Grothe et al. 1997; Watabe et al. 1995; Cheng et al. 1998). However, the migration of SCs takes a long time to lead to axon regeneration. One alternative strategy to nerve regeneration is cell therapy, whose aim is to replace, repair or enhance the biological function of damaged tissue.

Over the last several years, the relatively recent discovery of neural precursors, i.e., adipose tissue-derived stem cells (ADSCs), in adult nerve injury has raised hopes for improving the limited recovery that occurs following stroke, spinal cord injury or PNI (Zuk et al. 2002; Chan et al. 2014). ADSCs can self-renew with a high growth rate and differentiate along several mesenchymal tissue lineages, including adipocytes, myocytes, chondrocytes, endothelial cells and Schwann-like cells (Zuk et al. 2001; Kingham et al. 2007; Nakagami et al. 2006). ADSCs expressed various receptor tyrosine kinases (RTK), including ErbB2, TGF-β, and FGF1 receptors, which have potential to differentiate into Schwann-like cells (Scis) via treatment with PDGF, bFGF, foskolin, and neuregulin (Nrg1) (Scioli et al. 2014; Jiang et al. 2008). The transplantation of Scis differentiated from ADSCs provided the potential for Scis to

myelinate axons of neurons in vitro (Zuk et al. 2002), which could ultimately provide a therapeutic strategy for peripheral nerve repair.

In mammals, N-acetylgalactosaminyltransferase (GALNT) is widely expressed in nervous tissue and initiates the elongation of mucin type O-glycans on membrane proteins for nervous system development (Lin et al. 2008). In addition, many studies have indicated that mucin-type O-glycosylation plays a crucial role in a variety of biologic functions, such as angiogenesis, carcinogenesis, or neurogenesis (Wu et al. 2011; Herr et al. 2008; Lin et al. 2008).

The functions of O-glycosylation in ADSCs differentiation and peripheral nerve regeneration are largely unknown. We hypothesized that changes in O-glycosylation could regulate ADSC differentiation into Scis via the Neuregulin/ErbB2 pathway and mediate peripheral nerve regeneration.

To study the roles of mucin-type O-glycans in ADSC differentiation, we analysed the expression of O-glycosyltransferases in ADSCs using a quantitative polymerase chain reaction (PCR) approach. During cell differentiation, ADSCs were treated with an O-glycan inhibitor, benzyl-α-GalNAc, to suppress differentiation into Scis, acting as a negative control. To identify the role of ErbB2 receptor glycosylation in ADSCs, a lectin pull-down assay was used to examine the changes in the O-glycans on the growth factor receptors (ErbB2) of ADSCs. Furthermore, we transplanted ADSCs or ADSCs-differentiated Schwann-like cells into an end-to-end neurorrhaphy (EEN) rat model to evaluate the effects of ADSC-derived cells on peripheral nerve regeneration.

Materials and Methods

Isolation and culture of Adipose-derived stem cells

Adipose tissue containing ADSCs was obtained from rat inguinal and gonadal parts. Later, adipose tissue was treated with 0.1% collagenase type I (Gibco) at 37°C for 90 min, and clarified by centrifugation. Cells were then cultured with 10% foetal bovine

serum (FBS, Gibco). After changing the medium, rat ADSCs were passaged 3–5 times before use. The ability of adipogenic differentiation was confirmed by Oil-Red O (Sigma-Aldrich, USA) staining. The obtained ADSCs were induced into Schwann-like cells (Scis) with induction culture medium containing 10% FBS and the trophic factors of 14 mM forskolin (Sigma-Aldrich, USA), 10 ng/ml recombinant human basic fibroblast growth factor (Peprotech, USA), 5 ng/ml platelet-derived growth factor-BB (Peprotech, USA), and 200 ng/ml heregulin-1 β1 (Neuregulin 1; Nrg1, Peprotech, USA) for fourteen days (Liu et al. 2013; Reichenberger et al. 2015; New et al. 2015). Benzyl-α-N-acetylgalactosamine (benzyl-α-galnac, Sigma-Aldrich, USA) was used to inhibit the mucin-type O-glycosylation (Yoon et al. 1996). ADSCs were treated with benzyl-α-galnac to suppress their differentiation into Scis, acting as a disproof experiment. DiI stain (1,1'-Dioctadecyl-3,3,3'3'- Tetramethylindocarbocyanine; Sigma-Aldrich, USA) was used to track ADSCs and Scis at the site of repaired nerve (Weir et al. 2008).

Immunofluorescence staining

To identify the differentiation of ADSCs into Scis, Schwann cell markers, including S-100 and glial filament acidic protein (GFAP), were used. The differentiated ADSCs, cultured on coverslips, were fixed in 4% paraformaldehyde for 10 min and permeabilized with the blocking medium containing 0.1% Triton X-100, 3% normal goat serum and 2% bovine serum albumin (all from Sigma-Aldrich, St. Louis, MO, USA) for 1 h to block nonspecific binding. Anti-glial filament acidic protein antibody (GFAP, mouse monoclonal, 1:400, Chemicon, USA) and Anti-S100 antibody (1:400, rabbit polyclonal Sigma-Aldrich, USA) were added and incubated overnight at 4°C. After incubation in the primary antibody, the sections were further incubated with FITC conjugated anti-mouse IgG and Cy3-conjugated anti-rabbit IgG (1:200; Jackson Immuno-Research, West Grove, PA, USA). Secondary antibodies were incubated with the cells at room temperature for 1 h. Cell nuclei were labelled with Hoechst 33342

(1:1000, Thermo Fisher Scientific, USA) for 30 min. Finally, the cells were observed under a confocal fluorescence microscope (SP5, Leica Microsystems, Wetzlar, Germany).

Quantitative Real-Time PCR

To investigate the potential role of the *GALNT* gene family in ADSC, we first analysed *GALNT1-14* and *GALNTL1-L6* expression in ADSCs by real-time RT-PCR. The quantitative PCR system, Mx3000P (Stratagene), was used to analyse gene expression in human ADSCs according to the manufacturer's protocol. In short, the reaction was conducted in a 25-μl volume consisting of 2 μl of cDNA, 400 nM each of sense and anti-sense primers and 12.5 μl of Brilliant SYBR Green QPCR Master Mix (Stratagene). The primers used in the reaction are indicated in Table 1. The PCR reactions were incubated at 95°C for 15 min, followed by 40 amplification cycles with 30 sec of denaturation at 95°C, 50 sec of annealing at 58°C and 30 sec of extension at 72°C. Samples were analysed in triplicate, and the product purity was checked by the dissociation curves at the end of real-time PCR cycles. The PCR products were confirmed to be correct by DNA sequencing. The relative quantity of specific gene expressions was normalized to *GAPDH* and analysed using the MxPro Software (Stratagene).

Table 1 Primers

GALNT1-S	atggcccagttacaatgctc	*GALNT1-AS*	atatttctggcagggtgacg
GALNT2-S	aaggagaagtcggtgaagca	*GALNT2-AS*	ttgagcgtgaacttccactg
GALNT3-S	aaagcgttggtcagcctcta	*GALNT3-AS*	aacgagaccttgagcagcat
GALNT4-S	tgctggcgtttttaacagtg	*GALNT4-AS*	tcctcgttgagctggagttt
GALNT5-S	tgacttaagggctcccattg	*GALNT5-AS*	atcagggatgggggctatac
GALNT6-S	tgggagctgtcacttcactg	*GALNT6-AS*	cctgtttcctgaggagcttg

GALNT7-S	tcttacgcagtttgctggtg	*GALNT7-AS*	ttcaacatgaggccatggta
GALNT8-S	gagcttagcctgagggtgtg	*GALNT8-AS*	ccaggccaagtagaccatgt
GALNT9-S	aacgtgtacccggagatgag	*GALNT9-AS*	cttggagtcaggcaagaagg
GALNT10-S	acagccaggtaatgggtgag	*GALNT10-AS*	gaagatgggatggcttttca
GALNT11-S	tgcttatcagtgaccgcttg	*GALNT11-AS*	acactgtgcactgtccgaag
GALNT12-S	catcttgcaggaggatggat	*GALNT12-AS*	ctggctccacagtctccttc
GALNT13-S	catctatccggactcccaga	*GALNT13-AS*	tcggttcggatttctttgtc
GALNT14-S	ctgagatgcacactgctggt	*GALNT14-AS*	catttcaccttgggcaactt
GALNTL1-S	gagctctccttcagggtgtg	*GALNTL1-AS*	cacttctgcagtgcgcttag
GALNTL2-S	ctctgtggtggctctgttga	*GALNTL2-AS*	atgtccgacaacccagtctc
GALNTL3-S	cctctggttagggtgcacat	*GALNTL3-AS*	gctaggtcagcatcgtcaca
GALNTL4-S	ccagaaccgcaagtctaagc	*GALNTL4-AS*	cactaacctggttccccaga
GALNTL5-S	cttgggcatcgaaagagaag	*GALNTL5-AS*	ttcgtgacactggacatggt
GALNTL6-S	gcagcaaatctctgtgtgga	*GALNTL6-AS*	caaagcagaatttccgggta
GFAP-S	aggaagattgagtcgctgga	*GFAP-AS*	atactgcgtgcggatctctt
S100-S	caggaattcatggcctttgt	*S100-AS*	gctggaaagctcagctccta
GAPDH-S	cttcaccaccatggagaa	*GAPDH-AS*	aggcagggatgatgttct

Lectin pull down and immunoprecipitation

To detect glycoproteins decorated with glycans, Jacalin agarose beads (Vector Laboratories, CA, USA) were used. Briefly, cell lysates (0.5 mg) were incubated with Jacalin agarose beads overnight at 4°C. The precipitated proteins were subjected to western blotting. Immunoprecipitates were analysed by western blotting using the anti-ErbB2 antibody. The ErbB2 receptors were O-glycosylated on rat ADSCs and the Huh7 cell line (hepatocellular carcinoma cell line).

Western blot analysis

The O-glycoproteins were purified on Jacalin beads before used. The antibodies against total ErbB2 (Cell Signaling Technology) and β-actin (BD Biosciences, USA) were used at 4°C overnight. After incubation with the primary antibodies, the membranes were incubated with horseradish peroxidase-conjugated secondary antibodies (Bethyl Laboratories, USA) at a dilution of 1:10000 for 1 h at room temperature. The immunoreaction was visualized with ECL solution (Millipore, Temecula, CA, USA), followed by 2 min of film exposure.

Experimental animals

Young, adult, male Wistar rats weighing 200-300 g (n = 18) obtained from the Laboratory Animal Center of Chung-Shan Medical University were used in this study. All experimental animals were housed under the same conditions with controlled temperature and humidity. For the care and handling of all experimental animals, the Guide for the Care and Use of Laboratory Animals (1985) as stated in the United States NIH Guidelines (NIH publication no. 86-23) were followed. All experimental procedures with adipose-derived stem cell (ADSC) implantation and end-to-end neurorrhaphy (EEN) were approved by the Laboratory Animal Center Authorities of Chung Shan Medical University (IACUC Approval No 1760).

Microsurgery and cell implantation

The in vivo model of PNI was performed by end-to-end neurorrhaphy (EEN), as described in our previous studies (Chang et al. 2013; Liao et al. 2009, 2010). Briefly, after deep anesthetization with an intraperitoneal injection of 7% chloral hydrate (Sigma-Aldrich, St. Louis, MO, USA), rats were placed on the surgical microscope, and an incision was made along the left mid-clavicular line to expose the left brachial plexus. Then, the musculocutaneous nerve (McN) was transected at the margin of the pectoralis major muscle. The end of the proximal ulnar nerve (UN) was then neurorrhaphied to the end of the distal McN (Oberlin et al. 1994) with 10-0 nylon

sutures (Ethilon, Edinburgh, UK) under a surgical microscope. All operated animals were divided into four groups.

These animals were divided into three treatment groups: Group I (n = 6) was subjected to EEN and then received PBS as a negative control group. Group II (n = 6) was subjected to EEN and then injected with1 µl of ADSCs. Group III (n = 6) was subjected to EEN and then injected with 1 µl of Scis. For ADSC and Schwann-like cell implantation, 1 x 10^5 cells were suspended in 1 µl of medium and injected into the nerve at the suture site. The skin wound was closed with 5-0 silk, and animals were kept for one and three months following the surgery.

Compound muscle action potential recording

To confirm nerve reconstruction recovery, compound muscle action potentials (CMAPs) of the repaired nerve and target muscle were recorded with a PowerLab electromyogram (AD instrument, Sydney, Australia). First, the experimental animals were anaesthetized. The stimulating electrode was placed above the reconnection site, and the recording electrode was placed in the biceps brachii muscle at the mid-humerus level. The recording electrode was kept 1 cm from the stimulating electrode with a piece of 5-0 nylon suture. The rat's tail was connected to the signal ground. Next, the nerve was stimulated with a 0.2-ms square pulse current at 2 mA and a repetition rate of 0.2 Hz. In sham-operated rats, electrodes were set at corresponding locations of the McN and biceps brachii muscle. The data were then digitized and analysed.

Perfusion and Tissue Preparation

At the end of the survival period after EEN, half of the experimental animals from all groups were deeply anesthetized with 7% chloral hydrate (0.4 mL/100 g) and subjected to transcardiac perfusion with 100 mL of Ringer's solution, followed by 45 min of fixation with 4% paraformaldehyde in 0.1 M phosphate buffer (PB), pH 7.4. After perfusion, the distal end of the repaired nerve was removed under a dissecting

microscope and kept in a similar fixative for 2 h. The tissue block was then immersed in graded concentrations of sucrose buffer (10-30%) for cryoprotection at 4°C overnight. Serial 25-μm-thick sections of the nerve segment were cut longitudinally with a cryostat (CM3050S, Leica Microsystems, Wetzlar, Germany) on the following day.

Statistical Analysis

All quantitative data acquired from spectrometric, immunofluorescence, immunoblotting and *assessments* of *action potential* in PBS-treated, ADSC-treated, and Sci-treated rats were subjected to Student's *t* test. Data were presented as the mean ± SD. $P < 0.05$ was considered statistically significant.

Results

Expression of GALNT family genes in rat primary ADSCs

We first explored the expression of O-glycosyltransferases in rat primary ADSCs by real-time RT-PCR. Among these genes, *GALNT1* and *GALNT2* were highly expressed in ADSCs, *GALNT10, GALNT11, GALNT12* were moderately expressed, and the other genes were detected at relatively low levels (Fig. 1).

Comparing both *GALNT1* and *GALNT2*, the mRNA expression level of *GALNT1* was twice as high as that of *GALNT2*. The average expression level of *GALNT1* mRNAs was three times higher than those of *GALNT10, GALNT11*, and *GALNT12*. The average expression level of the other GALNT mRNAs was seven times lower than that of *GALNT1* and *GALNT2*.

The outcome indicated that *GALNT1* gene plays a more dominant role in the expression of O-glycosyltransferases in ADSCs of rats and that *GALNT1* was the major gene.

ADSC differentiation into Scis is blocked by O-glycosylation inhibitor

To investigate whether O-glycosylation plays a role in the pathway of ADSCs differentiation, an O-glycosylation inhibitor was used. The results showed that the mRNA expression of GFAP in benzyl-α-GalNAc-treated Scis was 30-fold lower than

that of DMSO-treated Scis 2 weeks after differentiation. Furthermore, the mRNA expression of S100 in benzyl-α-GalNAc-treated Scis was 15-fold lower than that of DMSO-treated Scis (Fig. 2). These results suggest that O-glycosylation participates in ADSCs differentiation pathway into Scis and that blocking the synthesis of O-glycans by benzyl-α-GalNAc severely inhibits this mechanism in vitro. The presence of O-glycosylation must promote ADSC differentiation into Sci.

Alteration of glycosylation onErbB2 is involved in ADSC cell differentiation

To explore the existence of ErbB2 receptors on ADSCs and the presence of O-glycans, plant lectin was used to conjugate to different moieties, such as Jacalin beads, which have a high affinity for glycans containing the N-acetylgalactosamine (GalNAc) of glycosylated proteins. The strong affinity between lectin and its conjugate glycans allowed the isolation of glycoproteins from cell extracts.

Our results show that protein glycosylation differs considerably between pluripotent ADSCs and non-pluripotent Huh7 cells and demonstrate that lectin may be used as a biomarker to monitor pluripotency in stem cell populations. ADSCs expressed much higher levels of glycans attached to the glycoprotein, ErbB2, thus contributing to cell differentiation.

ADSC differentiation into a Schwann cell phenotype

To determine the morphologic features of these Schwann-like cells, immunofluorescence staining was performed by using antibodies against GFAP and S100, which are widely known markers for Schwann cells. In induced ADSCs, *60* % of the cells tested positive for Schwann cell markers, compared to 0.8% of the uninduced ADSC cells, at 14 days postinduction. Schwann-like cells had a bipolar-shaped morphology with long process projections on opposing sites (Fig. 4).

Immunocytochemistry showed that ADSCs expressed no existing markers of S-100 or GFAP, whereas Schwann-like cells differentiated from ADSCs expressed both S-100

and GFAP. The characteristics of the differentiated ADSCs were similar to those of genuine Schwann cells. However, this model was in vitro and was thus different from the exact conditions in vivo, in which Scis would not express a spindle shape. Instead, Scis in vivo would myelinate around axons.

Forelimb functional recovery evaluation

In the present study, we employed end-to-end neurorraphy (EEN) as an in vivo model to detect the possible effects of ADSC on facilitating nerve regeneration. Compound muscle action potentials were recorded at the biceps brachii 1 month following EEN. A functional evaluation of the normal control group was shown in our previous study (Liao et al. 2009). The beneficial effect of Scii on facilitating nerve regeneration was validated by electrophysiological recordings, in which the regenerated axons successfully re-innervated the target muscles and generated higher CMAPs with an 11 mA stimulus (5.3 ± 0.5 mV vs. 2.5 ± 0.3 mV vs.2.15 ± 0.25 mV in Scii-, ADSC-, and PBS-treated groups, respectively) after EEN (Fig. 5). However, the ADSC-treated group did not show any significant differences compared to the PBS group. The amplitudes of the CMAPs in the Scii-treated groups with a 5 mA stimulus were slightly higher than those of the PBS group (2.1 ± 0.1 vs. 1.2 ± 0.08 mV vs. 1.1 ± 0.05 mV in Scii, ADSC, and PBS treated groups, respectively). Stronger stimuli evoked slightly larger amplitudes of CMAPs and showed more improvement of the responses in the Scii-treated groups. The results indicated that rats transplanted with Scis at the suture sites had a better functional nerve repair outcome when they were given a stronger stimulus compared to the ADSC- and PBS-treated groups.

Allogeneic Scis transplantation and survival

One month after EEN, the repaired nerve was evaluated histologically. CM-DiI dye was used to identify and track the existence of transplanted Scis in the suture site of the repaired nerve. No significant effects on allograft survival were found in either the

ADSC- or Scis-treated groups. Immunofluorescence photomicrograph showed that grafted Scis, labelled in red (Fig. 6 arrow), lived and surrounded the suture sites of the reconnected nerves at one month following transplantation. This outcome supported the concept that Scis were able to migrate into the reconstructed area, which was the main property for peripheral nerve repair. Schwann-like cells can thus effectively repair a damaged nerve in EEN rats.

Discussion

The present study was the first to report that O-glycan participated in the neural differentiation of ADSC into Scis in a nerve repair model. The mRNA expression of the *GALNT* family was shown in rat ADSCs. We documented the mRNA level of *GALNT1* and *GALNT2*, both of which were abundantly expressed in ADSCs compared to the other GALNT genes. The O-glycosylation of ADSCs was mainly processed by *GALNT1* family genes. Furthermore, we show that O-glycosyltransferases regulated ADSC differentiation via ErbB2 and blocked the induction of Scis by benzyl-α-GalNAc. In this regard, we found that with the addition of an O-glycosylation inhibitor, the S100/ GFAP expression of ADSC group treated with benzyl-α-GalNAc was reduced to a level lower than that of the control group, which was treated with DMSO. The outcome suggested that blocking the synthesis of O-glycans with an inhibitor of mucin glycosylation severely inhibited ADSCs differentiation into Scis in vitro.

Regulation of ADSC differentiation into Scis by glycosylation on ErbB2

In the present study, we used lectins as biomarkers to distinguish pluripotency in ADSC populations from other cell populations. In the *l*ectin pull-down assay, the expression of O-glycosylated ErbB2 protein on pluripotent ADSCs was higher than that of the non-pluripotent Huh7 cell line. Furthermore, the result indicated that ErbB2 receptors are indeed O-glycosylated, exist on the surface of ADSCs and mediate the differentiation of ADSCs into Scis.

In previous study, ErbB3 has been considered as a “kinase-dead” receptor (Boudeau et al. 2006; Citri et al. 2003). Thus, ErbB2 is the most important one leads to the activation of pathway which lead to adipogenic cell differentiation (Cervelli et al. 2012; Lee et al. 1995; Naderi et al. 2017)**.** We found that GALNT1 was a key enzyme that mediated ErbB2-regulated pathway in early stages of ADSC differentiation.

However, the ratio of Schwann cell differentiation of adipose-derived stem cells was reduced by benzyl-α-GalNAc. We suggested that the loss of an O-glycans-modulating cell signalling event could influence the post-translational modifications of the ErbB2 during SCi development. Similar findings were also observed in E Tian’s study. The loss of an O-glycosyltransferase (GALNT1) causes pronounced effects on organogenesis and cell proliferation by disrupting integrin and FGF signalling during early submandibular gland development (Tian et al. 2012).

It is known that the Nrg1/ErbB signal is involved in the fate of early Schwann cell development (Newbern and Birchmeier 2010; Yarden and Sliwkowski 2001). Our findings suggested that O-glycosyltransferase (GALNT1) modified the carbohydrate moieties on the ErbB2/ErbB3 heterodimer to alter the binding affinity of ErbB to its ligand. Furthermore, ADSC successfully differentiated into Scii via their key glycosylation state. This work provides the first evidence that the loss of O-glycans can alter receptor tyrosine kinase signalling by influencing the ErbB2 response to Nrg1 and stem cell differentiation.

Scis responses to the end-to-end neurorrhaphy model

In this research, we found that changes in O-glycosylation could regulate ADSC differentiation into Scis via the Nrg1/ErbB pathway and could, in turn, promote peripheral nerve regeneration after EEN.

In addition to the in vitro experiments, differentiated Scis were transplanted onto the distal end of a repaired nerve in vivo. Not only did we track the distribution of the surviving Scis around the reconnected nerve axons by using DiI one month after EEN, but we also recorded the amplitude of the compound muscle action potentials of the biceps brachii contractions one month after EEN. Our results implicated that the Scis-treated group showed better functional recovery by triggering a 1.6-fold larger amplitude than that exhibited by the control rats.

Scis, when transplanted in an artificial nerve conduit, could stimulate the outgrowth of axons from the proximal nerve stump and trigger greater SC proliferation or intrusion in the distal stump (Hadlock et al. 2000). ADSCs alone could enhance peripheral nerve regeneration, but Scis had a greater capability to improve the number, density, and length of neurites per neuron, which implied more benefits when used to treat peripheral nerve injuries (di Summa et al. 2010; Kingham et al. 2007). In addition, the regenerative effects of transplanted ADSCs were possibly mediated by an initial boost of released trophic factors or by an indirect effect on endogenous SC activity(Erba et al. 2010). Therefore, the transplantation of Scis in peripheral nerve repair and regeneration could be more direct and time-saving than could using undifferentiated ADSCs. The reconstruction of peripheral nerve injuries is currently completed with nerve autografts (Millesi 1990). The transplantation of allogeneic donor SCs could result in tissue rejection, which in turn would be replaced by host SCs (Midha et al. 1994). However, allogenic SCs boosted the axonal regeneration and did not produce a deleterious immune response in vivo. Additionally, the SCs' ingrowth into the transplanted suture sites was not adversely affected by the process of tissue rejection. In spite of allogeneic SC rejection, the regeneration effects continued at the transplanted sites (Mosahebi et al. 2002). Owing to this characteristic of transplanted allogeneic SCs, the immediate availability of allogeneic SCs for transplantation could compensate for the use of

autologous SCs, which require a longer preparation time in culture. Therefore, to provide time-saving, easily accessible and efficient regeneration and repair in peripheral nerve injuries, large numbers of Scis should be differentiated from ADSCs for clinical use in years to come.

Conclusions

This study revealed that O-glycosyltransferases, such as GALNT1, are abundantly expressed in ADSCs and are essential for ErbB2 receptor glycosylation to promote ADSC into Sci cells. Blocking the synthesis of O-glycans by benzyl-α-GalNAc severely inhibited ADSCs differentiation into Schwann-like cells in vitro.

The present study showed the first functional evidence that mucin-type O-glycans participated in ADSCs-Schwann cell differentiation. The obtained information will not only improve our understanding of the process by which ADSCs differentiate into Schwann-like cells but also provide insight into the role of this conserved protein modification in peripheral nerve regeneration.

Figure Legends

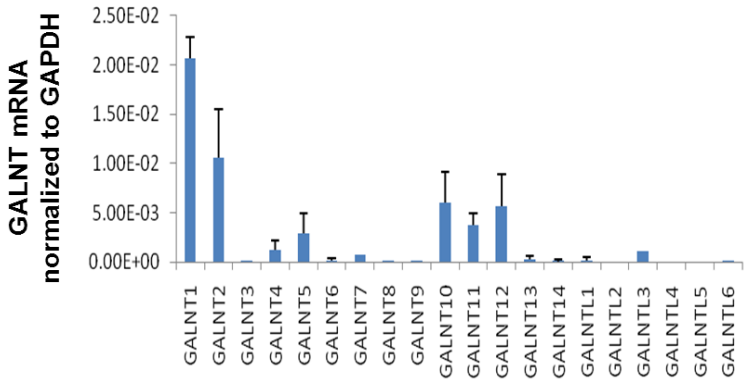

Fig. 1 GALNT gene expression in rat ADSCs.

Histogram showing the relative mRNA expression of the *GALNT* family in ADSCs by

quantitative real-time polymerase chain reaction (QPCR). The mRNA expressions of *GALNT* were normalized by *GAPDH* as a housekeeping gene. The experiment was done in triplicate, and the mean ± SD is shown.

Genes were divided into three groups according to the expression levels. *GALNT1* and *GALNT2* were highly expressed genes in ADSCs. *GALNT10*, *GALNT11*, and *GALNT12* were moderately expressed genes, and the other genes were detected at relatively low levels in ADSCs.

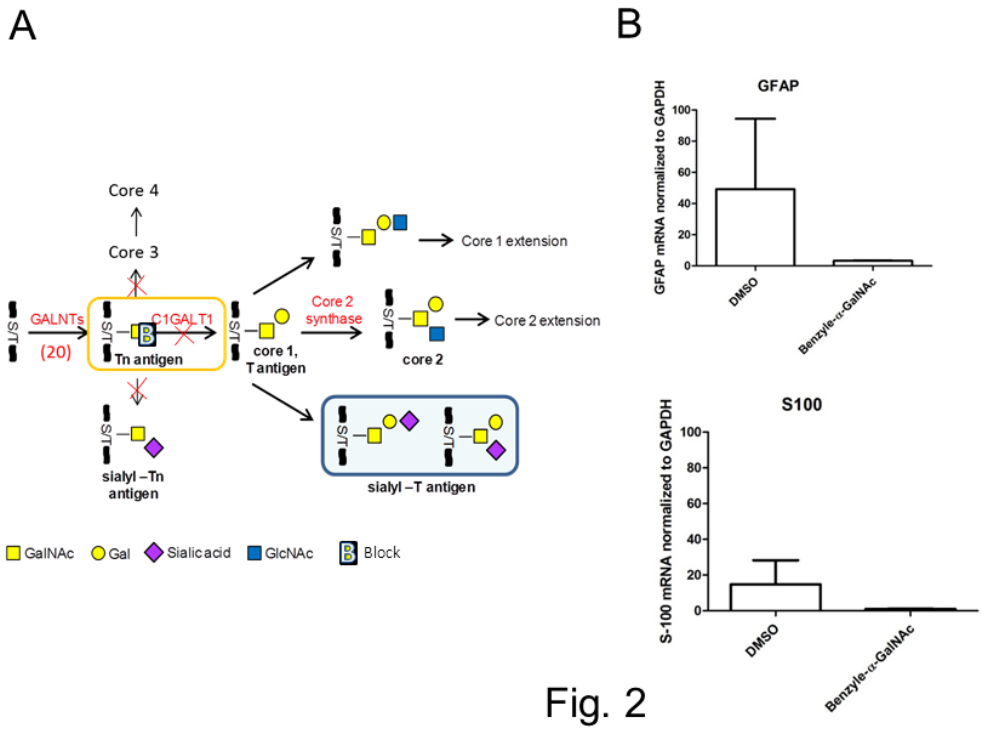

Fig. 2

Fig. 2 O-glycosylation inhibitor suppressed ADSCs into Schwann-like cells.

Representative diagram (A) showing O-glycan-extension reaction was blocked at T antigen of the glycan chains by O-glycosylation inhibitor such as benzyl GalNAc. Histogram (B) showing the relative mRNA of *GFAP* and *S100* expressed in benzyl-α-GalNAc-treated Scis and DMSO-treated Scis by quantitative real-time polymerase chain reaction (QPCR). The mRNA expressions of *S100/GFAP* were normalized by *GAPDH* as a housekeeping gene. The experiment was done in triplicate

and mean ± SD is shown. ADSCs were treated with an O-glycosylation inhibiter (2 mM; benzyl GalNAc) or DMSO for 2 weeks, respectively. Note that in both benzyl-α-GalNAc-treated Scis and DMSO-treated Scis, the mRNA level of *S100 and GFAP* was higher in DMSO-treated Scis than in benzyl-α-GalNAc-treated Scis, which suggests that glycosylation participated in the regulation of ADSC differentiation into Scii.

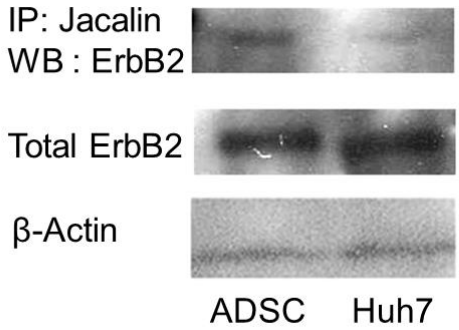

Fig. 3 Pull-down and western blotting analysis in ADSC and Huh7 cells.

ADSC and Huh 7 cell (hepatocellular carcinoma cell line) extracts were incubated with the anti-Jacalin beads overnight. Supernatants were separated from bead pellets by centrifugation and specific immunoblotting. Immunoprecipitates were analysed by western blotting using the anti-ErbB2 antibody. Actin was used as the loading control. ErbB2 protein glycosylation differed considerably between ADSCs and non-pluripotent Huh7 cells.

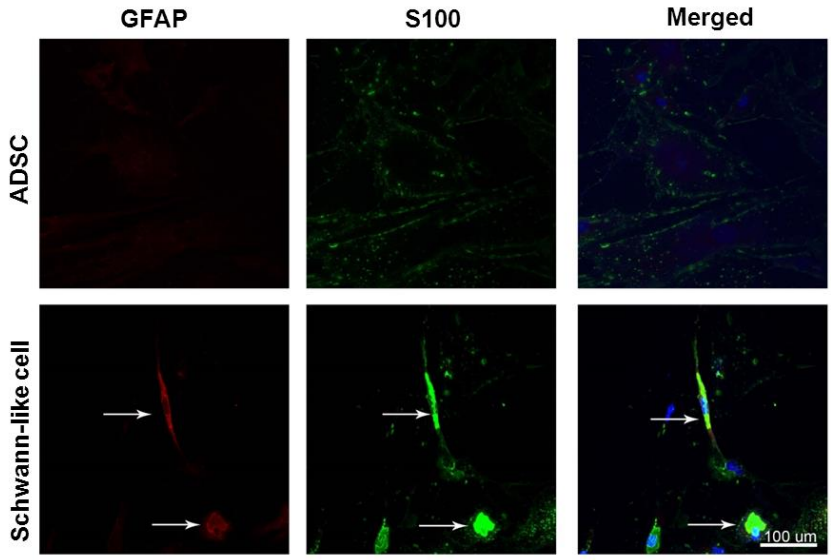

Fig. 4 Identification of Schwann-like cells.

ADSC was evaluated by immunofluorescence staining using Schwann cell markers *GFAP* and *S100* antibody. Immunofluorescence staining of *GFAP* (red) and *S100* (green). Cell nuclei were labelled with Hoechst 33342 (blue). Merged images show that the Schwann-like cells were positive for *GFAP* and *S100* (arrow).

GFAP/S100 double-labelled cells acquired elongated/spindle shape or round-shaped morphology. The round-shaped Schwann-like cells were cells not spread open. Scale bar = 100 μm.

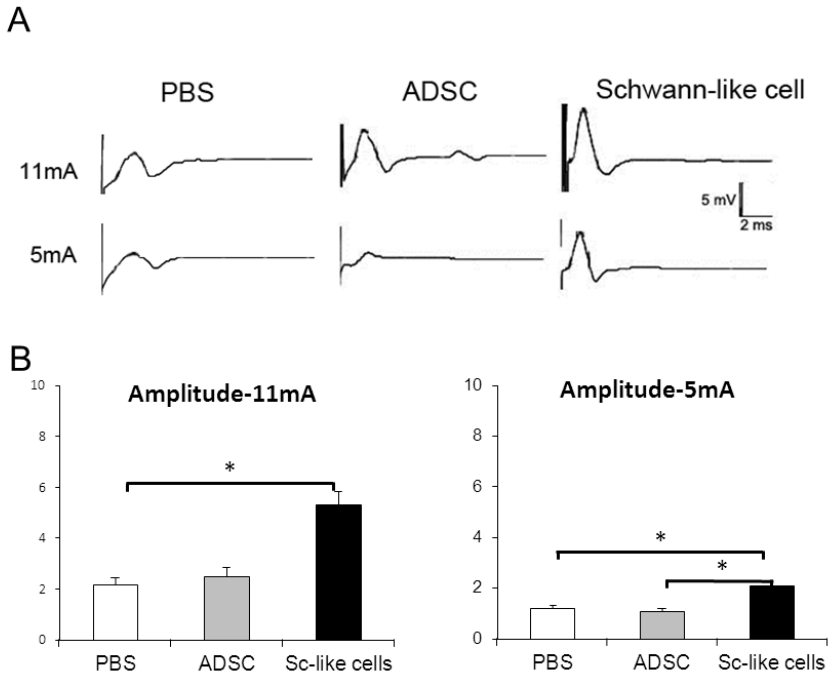

Fig. 5 Effects of cell implantation on compound muscle action potential recordings (CMAPs).

Representative CMAPs (A) showing action potentials recorded from the biceps brachii muscle upon activation of the musculocutaneous nerve one month following end-to-end neurorrhaphy (EEN). Responses were recorded from PBS-treated rats, ADSCs-treated rats and Schwann-like cell-treated rats with a stimulus applied above the neurorrhaphy site. Histogram (B) showing show the average amplitudes. $N = 6$ for each group. Values are the mean ± SD. $*P < 0.05$ compared to the PBS group. The Schwann-like cell-treated group promoted functional recovery by triggering a larger amplitude than that of the PBS group.

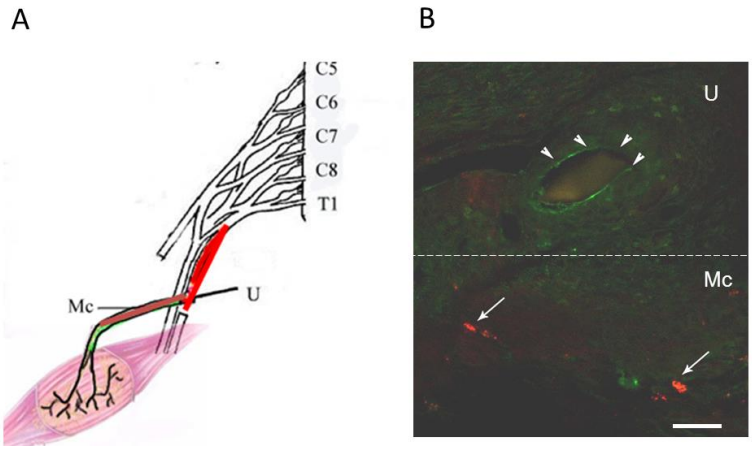

Fig. 6 DiI-labelled Schwann like cells in repaired nerve.

Schematic presentation (A) showing the microsurgery procedure of neurorrhaphied McN and UN. Confocal photomicrographs (B) showing the distribution of DiI (+) Scii. CM-DiI dye was applied in Schwann-like cells to label and track the reconnected nerve. We found that red Schwann-like cells (arrow) survived and presented at the suture site one month after EEN. Arrow head shows the 10/0 silk suture that was retained in the reconnected nerve. Scale bar = 50 μm U: ulnar nerve; Mc: musclocutaneous nerve.

Reference

Boudeau J, Miranda-Saavedra D, Barton GJ, Alessi DR (2006) Emerging roles of pseudokinases. Trends in cell biology 16 (9):443-452. doi:10.1016/j.tcb.2006.07.003

Carroll SL, Miller ML, Frohnert PW, Kim SS, Corbett JA (1997) Expression of neuregulins and their putative receptors, ErbB2 and ErbB3, is induced during Wallerian degeneration. J Neurosci 17 (5):1642-1659

Cervelli V, Scioli MG, Gentile P, Doldo E, Bonanno E, Spagnoli LG, Orlandi A (2012) Platelet-rich plasma greatly potentiates insulin-induced adipogenic differentiation of human adipose-derived stem cells through a serine/threonine kinase Akt-dependent mechanism and promotes clinical fat graft maintenance. Stem Cells Transl Med 1 (3):206-220. doi:10.5966/sctm.2011-0052

Chan TM, Harn HJ, Lin HP, Chiu SC, Lin PC, Wang HI, Ho LI, Chuu CP, Chiou TW, Hsieh AC, Chen YW, Ho WY, Lin SZ (2014) The use of ADSCs as a treatment for

chronic stroke. Cell transplantation 23 (4-5):541-547. doi:10.3727/096368914x678409

Chang HM, Shyu MK, Tseng GF, Liu CH, Chang HS, Lan CT, Hsu WM, Liao WC (2013) Neuregulin facilitates nerve regeneration by speeding Schwann cell migration via ErbB2/3-dependent FAK pathway. PLoS One 8 (1):e53444. doi:10.1371/journal.pone.0053444

Chen Z-L, Yu W-M, Strickland S (2007) Peripheral regeneration. Annual Review of Neuroscience 30:209-233

Cheng L, Esch FS, Marchionni MA, Mudge AW (1998) Control of Schwann cell survival and proliferation: autocrine factors and neuregulins. Mol Cell Neurosci 12 (3):141-156. doi:10.1006/mcne.1998.0706

Ciaramitaro P, Mondelli M, Logullo F, Grimaldi S, Battiston B, Sard A, Scarinzi C, Migliaretti G, Faccani G, Cocito D, Italian Network for Traumatic N (2010) Traumatic peripheral nerve injuries: epidemiological findings, neuropathic pain and quality of life in 158 patients. Journal of the peripheral nervous system : JPNS 15 (2):120-127. doi:10.1111/j.1529-8027.2010.00260.x

Citri A, Skaria KB, Yarden Y (2003) The deaf and the dumb: the biology of ErbB-2 and ErbB-3. Experimental cell research 284 (1):54-65

Davis JB, Stroobant P (1990) Platelet-derived growth factors and fibroblast growth factors are mitogens for rat Schwann cells. J Cell Biol 110 (4):1353-1360

di Summa PG, Kingham PJ, Raffoul W, Wiberg M, Terenghi G, Kalbermatten DF (2010) Adipose-derived stem cells enhance peripheral nerve regeneration. Journal of Plastic, Reconstructive & Aesthetic Surgery 63 (9):1544-1552. doi:http://dx.doi.org/10.1016/j.bjps.2009.09.012

Erba P, Mantovani C, Kalbermatten DF, Pierer G, Terenghi G, Kingham PJ (2010) Regeneration potential and survival of transplanted undifferentiated adipose tissue-derived stem cells in peripheral nerve conduits. Journal of Plastic, Reconstructive & Aesthetic Surgery 63 (12):e811-e817. doi:http://dx.doi.org/10.1016/j.bjps.2010.08.013

Evans GR (2001) Peripheral nerve injury: a review and approach to tissue engineered constructs. Anat Rec 263 (4):396-404

Grothe C, Meisinger C, Hertenstein A, Kurz H, Wewetzer K (1997) Expression of fibroblast growth factor-2 and fibroblast growth factor receptor 1 messenger RNAs in spinal ganglia and sciatic nerve: regulation after peripheral nerve lesion. Neuroscience 76 (1):123-135

Hadlock T, Sundback C, Hunter D, Cheney M, Vacanti JP (2000) A polymer foam conduit seeded with Schwann cells promotes guided peripheral nerve regeneration. Tissue engineering 6 (2):119-127

Herr P, Korniychuk G, Yamamoto Y, Grubisic K, Oelgeschläger M (2008) Regulation of TGF-(beta) signalling by N-acetylgalactosaminyltransferase-like 1. Development 135 (10):1813-1822

J W Faweett a, Keynes RJ (1990) Peripheral Nerve Regeneration. Annual Review of Neuroscience 13 (1):43-60. doi:doi:10.1146/annurev.ne.13.030190.000355

Jiang L, Zhu JK, Liu XL, Xiang P, Hu J, Yu WH (2008) Differentiation of rat adipose tissue-derived stem cells into Schwann-like cells in vitro. Neuroreport 19 (10):1015-1019. doi:10.1097/WNR.0b013e3283040efc

Kingham PJ, Kalbermatten DF, Mahay D, Armstrong SJ, Wiberg M, Terenghi G (2007) Adipose-derived stem cells differentiate into a Schwann cell phenotype and promote neurite outgrowth in vitro. Experimental Neurology 207 (2):267-274. doi:http://dx.doi.org/10.1016/j.expneurol.2007.06.029

Lee K-F, Simon H, Chen H, Bates B (1995) Requirement for neuregulin receptor erbB2 in neural and cardiac development. Nature 378 (6555):394

Liao WC, Chen JR, Wang YJ, Tseng GF (2009) The efficacy of end-to-end and end-to-side nerve repair (neurorrhaphy) in the rat brachial plexus. J Anat 215 (5):506-521. doi:10.1111/j.1469-7580.2009.01135.x

Liao WC, Chen JR, Wang YJ, Tseng GF (2010) Methylcobalamin, but not methylprednisolone or pleiotrophin, accelerates the recovery of rat biceps after ulnar to musculocutaneous nerve transfer. Neuroscience 171 (3):934-949. doi:10.1016/j.neuroscience.2010.09.036

Lin Y-R, Reddy BVVG, Irvine K (2008) Requirement for a core 1 galactosyltransferase in the Drosophila nervous system. Developmental dynamics 237 (12):3703-3714

Liu Y, Zhang Z, Qin Y, Wu H, Lv Q, Chen X, Deng W (2013) A new method for Schwann-like cell differentiation of adipose derived stem cells. Neuroscience Letters 551:79-83. doi:http://dx.doi.org/10.1016/j.neulet.2013.07.012

Midha R, Mackinnon SE, Becker LE (1994) The fate of Schwann cells in peripheral nerve allografts. J Neuropathol Exp Neurol 53 (3):316-322

Millesi H (1990) Progress in peripheral nerve reconstruction. World J Surg 14 (6):733-747

Mosahebi A, Fuller P, Wiberg M, Terenghi G (2002) Effect of allogeneic Schwann cell transplantation on peripheral nerve regeneration. Exp Neurol 173 (2):213-223. doi:10.1006/exnr.2001.7846

Naderi N, Combellack EJ, Griffin M, Sedaghati T, Javed M, Findlay MW, Wallace CG, Mosahebi A, Butler PE, Seifalian AM (2017) The regenerative role of adipose-derived stem cells (ADSC) in plastic and reconstructive surgery. International wound journal 14 (1):112-124

Nakagami H, Morishita R, Maeda K, Kikuchi Y, Ogihara T, Kaneda Y (2006) Adipose tissue-derived stromal cells as a novel option for regenerative cell therapy. Journal of atherosclerosis and thrombosis 13 (2):77-81

New SE, Alvarez-Gonzalez C, Vagaska B, Gomez SG, Bulstrode NW, Madrigal A, Ferretti P (2015) A matter of identity - Phenotype and differentiation potential of human somatic stem cells. Stem Cell Res 15 (1):1-13. doi:10.1016/j.scr.2015.04.003

Newbern J, Birchmeier C (2010) Nrg1/ErbB signaling networks in Schwann cell development and myelination. Seminars in cell & developmental biology 21 (9):922-928. doi:10.1016/j.semcdb.2010.08.008

Oberlin C, Beal D, Leechavengvongs S, Salon A, Dauge MC, Sarcy JJ (1994) Nerve transfer to biceps muscle using a part of ulnar nerve for C5-C6 avulsion of the brachial plexus: anatomical study and report of four cases. J Hand Surg Am 19 (2):232-237. doi:10.1016/0363-5023(94)90011-6

Papalia I, Geuna S, D'Alcontres FS, Tos P (2007) Origin and history of end-to-side neurorrhaphy. Microsurgery 27 (1):56-61. doi:10.1002/micr.20303

Reichenberger MA, Mueller W, Hartmann J, Diehm Y, Lass U, Koellensperger E, Leimer U, Germann G, Fischer S (2015) ADSCs in a fibrin matrix enhance nerve regeneration after epineural suturing in a rat model. Microsurgery. doi:10.1002/micr.30018

Scioli MG, Bielli A, Gentile P, Mazzaglia D, Cervelli V, Orlandi A (2014) The biomolecular basis of adipogenic differentiation of adipose-derived stem cells. International journal of molecular sciences 15 (4):6517-6526. doi:10.3390/ijms15046517

Son YJ, Thompson WJ (1995a) Nerve sprouting in muscle is induced and guided by processes extended by Schwann cells. Neuron 14 (1):133-141

Son YJ, Thompson WJ (1995b) Schwann cell processes guide regeneration of peripheral axons. Neuron 14 (1):125-132

Tian E, Hoffman MP, Ten Hagen KG (2012) O-glycosylation modulates integrin and FGF signalling by influencing the secretion of basement membrane components. Nature communications 3:869. doi:10.1038/ncomms1874

Tsai Y-T, Yu R (2014) Epigenetic activation of mouse ganglioside synthase genes: implications for neurogenesis. Journal of neurochemistry 128 (1):101-110

Viterbo F, Trindade JC, Hoshino K, Mazzoni Neto A (1992) Latero-terminal neurorrhaphy without removal of the epineural sheath. Experimental study in rats. Rev Paul Med 110 (6):267-275

Watabe K, Fukuda T, Tanaka J, Honda H, Toyohara K, Sakai O (1995) Spontaneously immortalized adult mouse Schwann cells secrete autocrine and paracrine

growth-promoting activities. J Neurosci Res 41 (2):279-290. doi:10.1002/jnr.490410215

Weir C, Morel-Kopp MC, Gill A, Tinworth K, Ladd L, Hunyor SN, Ward C (2008) Mesenchymal stem cells: isolation, characterisation and in vivo fluorescent dye tracking. Heart Lung Circ 17 (5):395-403. doi:10.1016/j.hlc.2008.01.006

Wu Y-M, Liu C-H, Hu R-H, Huang M-J, Lee J, Jr., Chen C-H, Huang J, Lai H-S, Lee P-H, Hsu W-M, Huang H-C (2011) Mucin glycosylating enzyme GALNT2 regulates the malignant character of hepatocellular carcinoma by modifying the EGF receptor. Cancer research 71 (23):7270-7279

Yarden Y, Sliwkowski MX (2001) Untangling the ErbB signalling network. Nature reviews Molecular cell biology 2 (2):127-137. doi:10.1038/35052073

Yoon WH, Park HD, Lim K, Hwang BD (1996) Effect of O-glycosylated mucin on invasion and metastasis of HM7 human colon cancer cells. Biochem Biophys Res Commun 222 (3):694-699. doi:10.1006/bbrc.1996.0806

Zuk PA, Zhu M, Mizuno H, Huang J, Futrell JW, Katz AJ, Benhaim P, Lorenz HP, Hedrick MH (2001) Multilineage cells from human adipose tissue: implications for cell-based therapies. Tissue Eng 7 (2):211-228. doi:10.1089/107632701300062859

Zuk PA, Zhu M, Ashjian P, De Ugarte D, Huang J, Mizuno H, Alfonso Z, Fraser J, Benhaim P, Hedrick M (2002) Human adipose tissue is a source of multipotent stem cells. Molecular biology of the cell 13 (12):4279-4295